

## Research Article

Christoph Schultheiss\*

# Theoretical and experimental clues to a flux of Doppler transformation energies during processes with energy conservation

<https://doi.org/10.1515/phys-2021-0088>

received April 17, 2021; accepted November 11, 2021

**Abstract:** In a microscopic model of the photoelectric effect, it becomes clear that the conservation of energy is exclusively determined by Doppler shift processes, *i.e.*, the whole energy of the photon vanishes by means of Doppler redshifts. Accordingly, if a photon is generated, the energy is won by Doppler blueshifts. This is supposed to be valid for all processes with energy conservation. An experiment is carried out to make this Doppler energy flow visible by means of interactions with probes. The result of this experiment is that a weak force is measurable in the vicinity of processes with energy conservation. With the aid of a twisted rubber-driven low-power device ( $\bar{P} = 10$  W), periodic accelerations and decelerations of about  $10^{-6}$  m/s<sup>2</sup> are measurable. In the close vicinity of the device, accelerations with values up to  $10^{-3}$  m/s<sup>2</sup> can be concluded. The consequences that result from this force are discussed.

**Keywords:** Compton effect, Doppler effect, energy-momentum conservation, flywheel

## 1 Introduction

The Doppler effect is investigated very well and is widely applied in science and technology. A particularly salient example of its applications is the Mößbauer effect [1], where velocities down to 1 mm/s are easily measurable.

Schrödinger [2] as well as other authors concluded that during a Compton collision between a charged particle and a photon the change of photon energy relates

exactly to a Doppler shift [3–7]. The shift corresponds to a direct increase or decrease of the wavelength in a red- or blueshift situation, respectively. However, the role of the Doppler shift in physics seems to go deeper as it appears at first glance. For example, Doppler and momentum equations alone solve all kinetic questions [8,9]. In this paper, I try to describe another new aspect of this kind of relativistic transformation.

## 2 Short derivation of the Compton shift as a Doppler shift

In Figure 1, let  $M$  be a big and  $m$  a small mass and both shall be charged particles. A photon reflects between both masses contained within ideally reflecting mirrors. In addition, the mirrors are aligned in parallel, so that the photon cannot escape during the reflections (see Figure 1). As a consequence of multiple reflections, the small mass  $m$  starts to accelerate away from the big mass  $M$  and the kinetic energy successively approaches  $\frac{1}{2}mv^2 \rightarrow hv$  [8,9], provided the lateral dimensions of the mirrors are unlimited. This is a model of the photoelectric effect proposed to be called the mirror mass model (MMM).

After the first collision with the photon, the small mass  $m$  moves with the velocity  $v_1 = \beta_1 \cdot c$  and the interacting photon, coming back from the moving charge, becomes Compton-shifted or Doppler-redshifted corresponding to  $\beta_1$ . This is demonstrated for the special case of an elastic 180° Compton collision.

With the abbreviations  $\alpha_0 = \frac{h\nu_0}{mc^2}$ ,  $\gamma_1 = (1 - \beta_1^2)^{-1/2}$  and for a system initially at rest ( $\beta_0 = 0$ ), the energy and momentum equations have the form equations (1) and (2). By mutual addition and subtraction of both energy and momentum conservation equations,

$$\alpha_0 + 1 = \alpha_1 + \gamma_1, \quad (1)$$

$$\alpha_0 + 0 = -\alpha_1 + \beta_1 \gamma_1, \quad (2)$$

\* Corresponding author: Christoph Schultheiss, Karlsruhe Institute of Technology (KIT), Institute for Pulsed Power and Microwave Technology (IHM), P.O. Box 3640, 76021 Karlsruhe, Germany, e-mail: eucschtul@yahoo.de

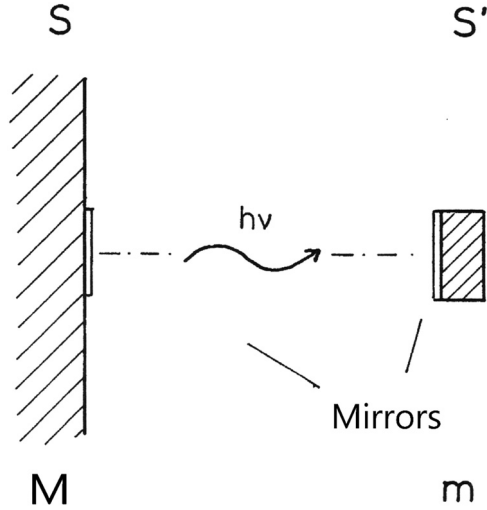


**Figure 1:** Arrangement of mirrors, masses and photon in the mirror mass model [8].

and using the defining equation  $\gamma_1 + \beta_1 \gamma_1 = (\gamma_1 - \beta_1 \gamma_1)^{-1}$ , this leads to the well-known solutions:

$$\alpha_1 = \alpha_0 (1 + 2\alpha_0)^{-1}, \quad (3)$$

$$\gamma_1 = 1 + 2\alpha_0^2 (1 + 2\alpha_0)^{-1}. \quad (4)$$

To make the Doppler mechanism visible, equations (1) and (2) can be rewritten as

$$\gamma_1 = \alpha_0 - \alpha_1 + 1, \quad (5)$$

$$\beta_1 \gamma_1 = \alpha_0 + \alpha_1. \quad (6)$$

Subtraction and addition lead to Doppler transformation-like expressions:

$$\gamma_1 - \beta_1 \gamma_1 = 1 - 2\alpha_1, \quad (7)$$

$$\gamma_1 + \beta_1 \gamma_1 = 1 + 2\alpha_0. \quad (8)$$

Using again the defining equation  $\gamma_1 + \beta_1 \gamma_1 = (\gamma_1 - \beta_1 \gamma_1)^{-1}$ , it follows that

$$\gamma_1 - \beta_1 \gamma_1 = 1 - 2\alpha_1 = (1 + 2\alpha_0)^{-1}. \quad (9)$$

Inserting this into equation (7) and comparing with equation (3), this gives

$$\gamma_1 - \beta_1 \gamma_1 = \frac{\alpha_1}{\alpha_0} \equiv D_1, \quad (10)$$

which is the Doppler equation with symbol  $D$ . The Compton shift is a Doppler shift. But, the role of the Doppler effect is still bigger: The hypothesis of ref. [8] demands: Any change

$$\alpha_2 = \underbrace{D_1}_{D_2} \underbrace{\tilde{D}_1}_{D_1} D_1 \cdot \alpha_1 = \underbrace{D_0}_{D_1} \underbrace{\tilde{D}_1}_{D_1} \cdot \tilde{D}_2 \cdot \underbrace{D_0}_{D_1} \underbrace{\tilde{D}_1}_{D_1} \cdot \underbrace{D_0}_{\alpha_1} \underbrace{\tilde{D}_1}_{D_0} \cdot \alpha_0 = \tilde{D}_2 \tilde{D}_1^3 D_0^4 \cdot \alpha_0, \quad \tilde{D}_2 = \frac{1}{1 + 2\alpha_0 D_0^2 \tilde{D}_1}, \quad (13b)$$

of photon energy is exclusively caused by Doppler transformation processes.

### 3 The DCAD method

Supported by the ladder statement, the Compton process can be decomposed into a number of single Doppler processes. The method to make this visible will be called DCAD. It stands for:

- Doppler transformation of the photon from system S into the moved system S' ( $D_{SS'}$ )
- Compton collision in the system S'; the system gains the Compton velocity ( $\tilde{D}$ )
- Addition (relativistic) of Compton and Doppler velocity gives the back-transformation velocity ( $\tilde{D} \cdot D_{S'S}$ )
- Doppler back-transformation of the photon from the system S' to the system S.

As seen from the system S in the arrangement of Figure 1, the sequence  $\alpha_0, \alpha_1, \alpha_2, \alpha_3$  and so on can be expressed in products of Doppler transformations. For example, the first turn has the form

$$\alpha_1 = D_{SS'} \cdot \tilde{D}_1 \cdot D_{S'S} \cdot \alpha_0, \quad D_1 \leq 1. \quad (11)$$

Here,  $D_{SS'}$  is the transformation of the photon from the system S into the system S'.

The term  $\tilde{D}_1$  is the Doppler shift coming from the Compton velocity, seen in the system S'. The velocity addition  $\tilde{D}_1 \cdot D_{S'S}$  stands for the back-transformation. Doppler shifts with the indexes S'S and SS' are equal in value and can in principle be written in equation (11) as  $D_0^2$ , which also means that the photon suffered two Doppler red-shifts – on the way from S to S' and the other one on the way back.

The Compton or Doppler shift  $\tilde{D}_1$  itself is defined in equation (10). The property  $\gamma_1$  is determined by equation (4) and  $\beta_1$  by means of the defining equation  $\beta_1(\gamma_1) = (1 - \gamma_1^{-2})^{\frac{1}{2}}$ , which gives finally

$$\tilde{D}_1 = \frac{1}{1 + 2\alpha_0}, \quad (12)$$

where  $\alpha_0$  is the photon energy in the frame S'. In the vein of equation (11), the first three collisions have the form

$$\alpha_1 = \underbrace{D_0}_{D_1} \underbrace{\tilde{D}_1}_{D_0} D_0 \cdot \alpha_0 = \tilde{D}_1 D_0^2 \cdot \alpha_0, \quad \tilde{D}_1 = \frac{1}{1 + 2\alpha_0}, \quad (13a)$$

$$\alpha_3 = \underbrace{D_2 \tilde{D}_3}_{D_3} D_2 \cdot \alpha_2 = \underbrace{D_0 \tilde{D}_1 \tilde{D}_2}_{D_2} \cdot \tilde{D}_3 \cdot \underbrace{D_0 \tilde{D}_1 \tilde{D}_2}_{D_2} \cdot \underbrace{\tilde{D}_2 \tilde{D}_1^3 D_0^4}_{\alpha_2} \cdot \alpha_0$$

$$= \tilde{D}_3 \tilde{D}_2^3 \tilde{D}_1^5 D_0^6 \cdot \alpha_0, \tilde{D}_3 = \frac{1}{1 + 2\alpha_0 D_0^4 \tilde{D}_1^3 \tilde{D}_2}$$

(13c)

In equation (13), the photon undergoes a series of energy changes in the fashion of a photoelectric effect process. This is a consequence of succeeding Doppler transformations of the form  $D_0^{2n} \cdot \tilde{D}_1^{2n-1} \cdot \tilde{D}_2^{2n-3} \cdot \tilde{D}_3^{2n}$ . For instance, the exponential growth  $D_0^{2n}$  indicates that initial Doppler shifts are repeated 2 times with each turn and so on.

Normally, Doppler transformations are considered to be a very intrinsic behavior of space-time. But, in the photoelectric effect, the Doppler mechanism does not appear explicitly in the energy and momentum conservation equations (see equations (1)–(4)), although the upper derivations clearly show the dominant role of Doppler transformations.

In Figure 2, the viewpoint of classical energy conservation *versus* the presented Doppler model of the photoelectric effect is sketched.

In the first case, by computation, all of the energy of the photon is transferred directly from the photon to the mass  $m$  in the form of kinetic energy. For reasons related to momentum, it is indispensable that in a photoelectric effect a heavy mass nearby must be involved to absorb the momentum. In the second case of Figure 2, an extra heavy mass is not necessary since the big mass  $M$  serves to reflect (absorb) the photon momentum without gaining kinetic energy (see Figure 1). The velocity of the small mass  $m$  changes step-wise to higher values. An observer in the system  $S'$  state that the photon coming from the

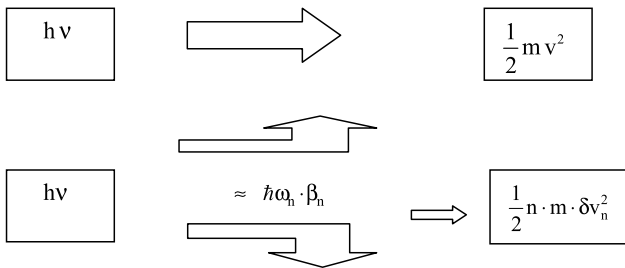


**Figure 2:** Classical scheme of energy transfer of a photon to a mass  $m$  during a photoelectric effect (upper panel), while in the microscopic model the flow of energy into the space is dominant in comparison with the direct step-wise flow on  $m$ . This is true especially in non-relativistic processes (see equation (14)). The mass  $m$  itself gains a velocity push ( $2\delta v_n$ ) with each collision and successively approaches the final velocity  $v$  after  $n$  reflections.

system  $S$  has lost energy by Compton redshift. The step-wise increase of velocity of the mass amounts in a non-relativistic case to  $\delta v = 2h/m\lambda$ . Particularly in the non-relativistic case, most of the photon energy “is absorbed” in the space by means of Doppler shifts. The quotient  $Q$  between the step-wise increase of kinetic energy and the loss due to red-shift shows that

$$Q = \frac{\frac{1}{2} \cdot m \cdot \delta v_n^2}{h\nu \left(1 - \frac{v_n}{c}\right) - h\nu} = \frac{\frac{1}{2} \cdot m \cdot \delta v_n^2}{h\nu \cdot \frac{v_n}{c}}$$

$$= \frac{\frac{1}{2} \cdot m \cdot \delta v_n}{m \cdot v_n} = \frac{1}{2} \cdot \frac{\delta v_n}{v_n}$$

$$= \frac{1}{2} \frac{\frac{h}{m \cdot \lambda_n}}{\sqrt{\frac{1}{2} \cdot \frac{hc}{m\lambda_n}}} = \sqrt{\frac{\delta v_n}{2c}} \rightarrow 0.$$

(14)

The smaller the  $\delta v_n$ , the bigger is the fraction of photon energy that is transferred into Doppler redshift energy. This is maximum in low-energy processes. The conclusion finally is: Each of these Doppler shift losses can be considered as the emission of something like transformation quanta (see Figure 2).

If we agree with the emission of a hypothetical Doppler transformation quantum (DTQ) into space, then it will take place during each photon reflection turn ( $S$  to  $S'$  and *vice versa*). The Taylor derivation in terms of  $\beta$  of equation (10) gives

$$h\nu' = h\nu \cdot D_i = h\nu \cdot \gamma'(1 - \beta'_i) = h\nu \frac{1 - \beta'_i}{\sqrt{1 - \beta_i'^2}}$$

$$= h\nu(1 - \beta'_i) \cdot \left(1 + \frac{1}{2}\beta_i'^2 - \frac{1}{8}\beta_i'^4 + \dots\right)$$

$$= h\nu - h\nu\beta'_i + \dots$$

(15)

The thesis is that  $h\nu$  decays in

$$h\nu \rightarrow h\nu' + \underbrace{h\nu \cdot \beta'_i}_{\text{DTQ}} + \dots,$$

(16)

where the relativistic term  $h\nu \cdot \beta'_i$  describes the DTQ mentioned above with the linear part of the Doppler effect. All higher terms in equation (16) are neglected, which have to do with different time reference systems  $M$  and  $m$ . It is obvious that the energy quantum DTQ is connected with the elementary quantum  $h$  such that DTQs can be assigned a wavelength. A rough calculation gives  $\lambda_{\text{DTQ}} \cdot \beta = \lambda_{\text{photon}}$ .

It is also obvious that in this formalism each photon carries the information about its emission and collision system. This is because the Doppler term in equation (16)

includes already the velocity difference  $\beta'$  between both systems. The question is – when does a Doppler shift happen: at the moment of the emission of the photon, in between or at the moment of the collision?

- (i) Let the Doppler shift take place in the course of emission; then the collision partner of the photon is already determined in advance, although the collision will take place anywhere (far) in the future. Irregular movements of the collision systems  $S'$  during flight time will complicate the situation.
- (ii) A Doppler shift anywhere between emission and collision increases the problem more. It needs information about the collision partner and the emission system too.
- (iii) The Doppler shift at the moment of collision in the system  $S'$  needs the knowledge of the emission system  $S$ .

An interesting aspect comes from an investigation of the Compton effect with a virtual mass hat built from a confined photon in a mirror cavity [9]. It turns out that the re-emission of the Compton photon takes place already in the form of a Doppler shifted recoil photon, although the laboratory system has not been entered yet. This means that the photon already knows how the transformation will look like. In this sense, following equation (16), after the emission, the photon has already decayed into a recoil photon and a DTQ. Both energy forms travel side by side until they become separated in the predetermined reflection of the photon. The DTQ – now on its own – continues the propagation in space and disappears finally in the DTQ pool.

In the opposite case, namely the absorption of space DTQs, the mass  $m$  moves in the direction of the mass  $M$ . The photon underlies a fusion with a space DTQ already at the emission and gains a reduced wavelength. However, in this case, a corresponding DTQ must move in the opposite direction to hold the neutrality of the space.

In this article, an accelerated metal mass is the source of DTQs. The question is: how an accelerated solid-state mass can produce DTQs. The imagination is that metal atoms built layers in a typical atomic distance. Between these layers, “binding photons” reflect back and forward hold the distance. Global acceleration, or deceleration, forces are transferred through the layers *via* electric binding fields from atom layer to atom layer until the outer force vanishes. The coupling process is accompanied by the emission and absorption of DTQs coming from the space or from the Doppler-shifted (binding) photons.

In the close vicinity of any collision process, the flux of DTQs should be measurable, if emitted or absorbed

DTQs have a finite cross-section for interaction with masses. This will be investigated and tested in an experiment described in Section 4.

## 4 The torsion balance measure system

The goal of the experiment is to detect very weak repulsive and attractive forces that appear periodically in the vicinity of an oscillating flywheel (see Section 4.1). Some basic assumptions must be discussed before. We assume a DTQ power-density  $j$  that should tangentially escape from or be absorbed by an accelerated or decelerated flywheel, respectively. The DTQs penetrate a probe mass nearby that shall consist of nucleons. The expected acceleration  $a$  of a nucleon that is penetrated by this flow can be estimated by means of the well-known formula in optics for radiation pressure in the case of total absorption of radiation:

$$a = \frac{\sigma j}{m_p c}. \quad (17)$$

The cross-section amounts to  $\sigma = 1.4 \times 10^{-2}$ ,  $b = 1.4 \times 10^{-30} \text{ m}^2$ , which corresponds to the area of a proton. For a power density of  $10^4 \text{ W/m}^2$ , an acceleration of about  $3 \times 10^{-8} \text{ m/s}^2$  can be expected.

### 4.1 Specification of the torsion balance and measure system

To measure weak forces, a sensitive torsion balance has been constructed. The torsion pendulum is of light plastic with a radius of 4.5 cm. On the one end of the pendulum, a lead–tin alloy is mounted and, on the other end, a small mirror is fixed with its surface directed normally to the radius (see Figures 3 and 5). The weight of each mass is 0.2 g. The total weight of the torsion balance is 0.5 g. The torsion balance is attached to a 27 cm long fibre of glass, with a diameter of  $1 \mu\text{m}$ , acting as a torsion wire. The restoring torque corresponds to  $2 \times 10^{-10} \text{ N/m}$ . The torsion oscillation time is about 6 min ( $1/2 T$ ). The torsion balance is installed in a glass container that can be evacuated down to 1 Pa. To shield the balance from thermal radiation and electrical fields, it was surrounded by some sheath of metallized plastic foil.

A weak light source – vertically positioned and small – is observed *via* a telescope with a focus of 90 cm from a

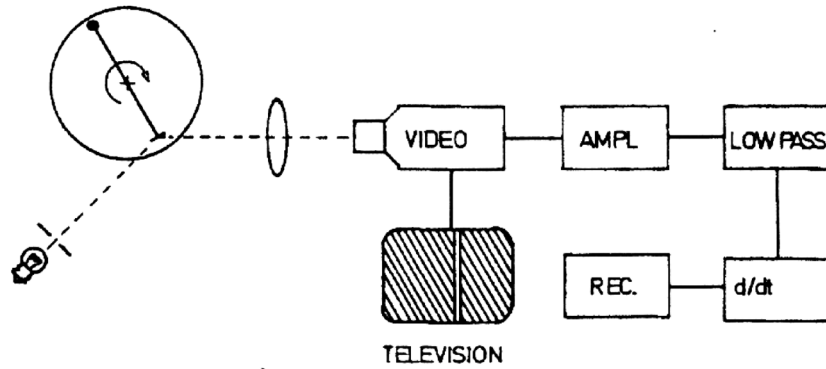


Figure 3: Scheme of the torsion balance measure system.

distance of 2.5 m (Figure 3). The movements of the pendulum are observed by a video camera, which is fixed at the end of the telescope, and the result is plotted by means of an  $x, t$ -recorder. By electronic methods, a linear electrical signal in reference to the position of the incident light-beam is obtained. The signal is smoothed out by means of an active three-step Tschebyscheff filter, with integration times between 0.5 and 4 s. To suppress signal shifts, generated by slow superpositioned movements of

the balance, the signal is finally differentiated by an R-C component to obtain the velocity and the direction of the rotation of the pendulum.

Figure 4 shows a test of the sensitivity of the torsion balance. The mutual gravitational attraction between a mass of 120 g and the masses of the torsion pendulum can be observed easily. The mass was positioned tangentially at a distance of 4 cm to one mass of the pendulum and then taken away. About 100 s later, the position of the mirror runs out of the detectable area of the measuring system described above. The calculated acceleration of the pendulum masses is about  $2 \times 10^{-9} \text{ m/s}^2$ . The

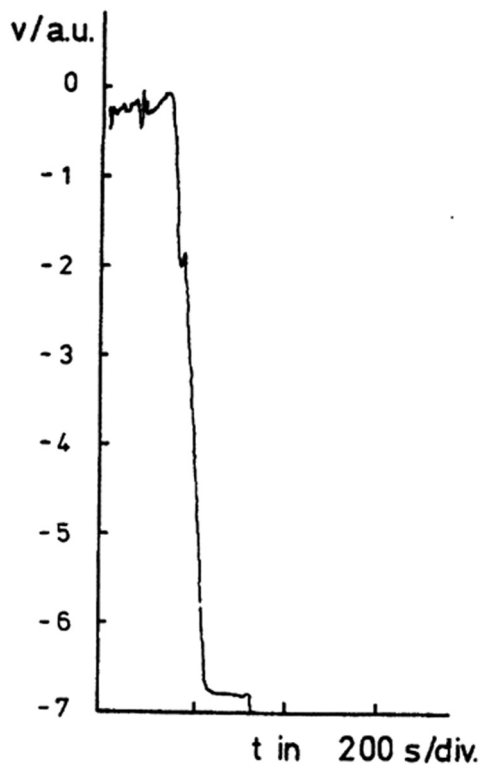


Figure 4: Sensitivity test of the torsion balance measuring system. A mass of 120 g, positioned near to one mass of the pendulum, was taken away. The fluctuation of the signal corresponds to accelerations of the order of  $10^{-11} \text{ m/s}^2$ .

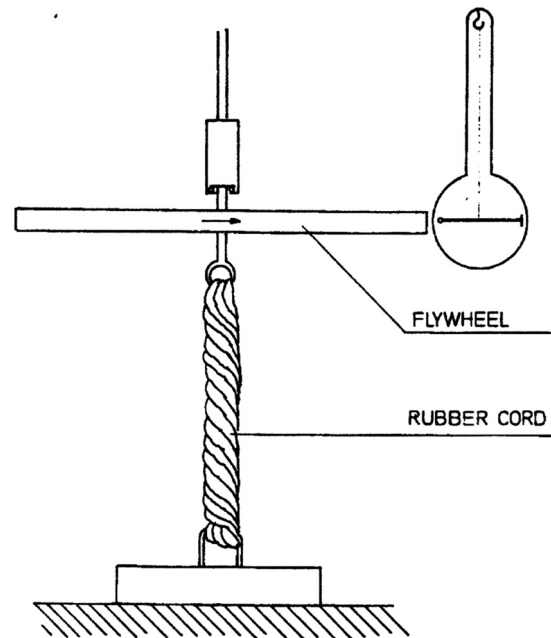


Figure 5: Side-view of the system made up of the flywheel and the torsion balance. The sense of rotation drawn indicates the initial movement of the flywheel, which is opposite to the final movement of the pendulum.

ratio between noise and signal in Figure 4 indicates a resolution limit in the range of  $10^{-11} \text{ m/s}^2$ , which corresponds to the gravitational force of a mass of  $\sim 1 \text{ g}$  in the position described above. Hence, the torsion balance has the potential to detect local DTQ power densities even if the cross-section is much smaller than  $10^{-5} \text{ b}$ .

## 4.2 Evidence for DTQs in the experiment

An optimal system to generate DTQ-related forces would be a device similar to the one presented in the MMM in Section 1 (see Figure 1). However, the light forces of a single photon or even an intense light beam are much too weaker to be of experimental use. So, one has to take, for instance, a mechanical oscillator and rely on the universality of the DTQ flow in energy conservation processes (see remarks at the end of Section 3). Since the expected forces are very weak and difficult to distinguish from small movements of a torsion pendulum, a periodic experiment was preferred. A DTQ-source with an

alternating tangential flow direction has the potential to detect effects even in noisy surroundings as long as a periodic structure of the signal can be stated.

### 4.2.1 Specification of the mechanical oscillator

The experimental set-up of the chosen mechanical oscillator is a flywheel of aluminium with a diameter of 48 cm, a thickness of 2 cm and a weight of 10 kg. The momentum of inertia is  $0.28 \text{ kg/m}^2$ . The drive of the flywheel is a cord of rubber fibres, 60 cm long and 3 cm in diameter. A sketch of the experimental set-up is shown in Figure 5. The rubber drive was chosen to avoid diamagnetic effects in the torsion balance caused by magnetic fields and radiometer forces, caused by, for instance, the thermal radiation of an electrical motor or a similar device. The torsion oscillation frequency of the flywheel amounts to 0.076 Hz. The disk of the flywheel was positioned in the same plane as the torsion pendulum (see Figure 5). The distance between the disk and the masses of the pendulum varied between 1 and 4 cm. The standard measure distance was 1 cm.

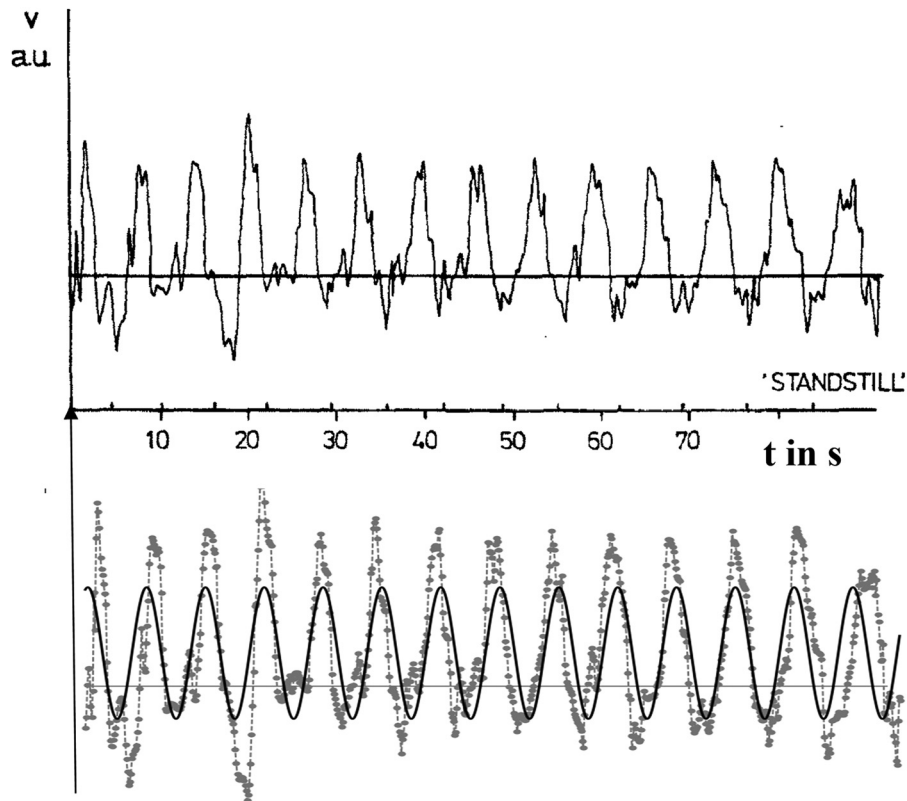


**Figure 6:** Periodical movement pattern of the torsion balance induced by tangential forces generated by the oscillating flywheel (upper panel). The markings at the horizontal time axis of the plot indicate the measured standstill of the flywheel. A sinus-fit on the data gives proof of the periodicity and the oscillation time (13.2 s). This even gives information about the sign of DTQ radiation. The resulting force effect is repulsive.

#### 4.2.2 Measurements

Before each measurement, the disk of the flywheel had been rotated completely 10 times and fixed in this position until the torsion balance was at rest. In each case, the torsion balance was filled with air. The gas pressure varies between 500 and 1,013 hPa mainly to suppress the radiometer forces. However, the force under study affects not only the mass of the pendulum but also the mass of the gas content in the glass vessel.

More distant positions between the flywheel and the pendulum mass show a roughly quadratic decreasing effect. Besides the metalized plastic foil that covered the glass vessel in some experiments, a 1 mm sheet of lead was fixed between the disk and the glass vessel. Statistically, no reduction of the effect was observed (Figure 6).

#### 4.2.3 Discussion of the measured signals

Figure 7 shows in principle – vertically arranged – the velocity of the pendulum mirror (here approximated by a  $\sin(\omega t)$ -function), the sign and intensity of the acting force on the low-distant pendulum mass (mirror), the angular velocity  $\omega$  and the angular acceleration  $\dot{\omega}$  over a whole oscillation period of the flywheel.

The force  $F$  can be interpreted as

$$F \propto \omega \cdot \dot{\omega} \quad (18)$$

depending not only on the angular acceleration  $a$  that the mass particles experience in the flywheel ( $\dot{\omega}$ ) but also on the actual angular velocity ( $\omega$ ) of the mass particles. A reasonable ansatz for the force seems to be

$$F = \text{const} \cdot f(r) \cdot a \cdot v, \quad (19)$$

where  $f(r)$  is the distance law (see Section 4.2.2),  $a$  is the average acceleration of the mass points in the flywheel and  $v$  is the average velocity of the mass points of the flywheel.

Equation (20) follows from equation (17) if  $j$  is substituted:

$$F = F_0 \frac{\sigma}{A} \cdot \frac{v}{c}, \quad (20)$$

Here,  $\sigma/A$  represents the distance law and  $v/c$  is the relativistic factor.

The average tangential force, that is, the average tangential acceleration of a mass particle in the outer radius of the flywheel, was estimated to be  $5 \text{ m/s}^2$  and the average velocity to be  $2 \text{ m/s}$ . Equation (20) yields an acceleration – corresponding to  $F$  – of the order of  $3 \times 10^{-8} \text{ m/s}^2$ . The

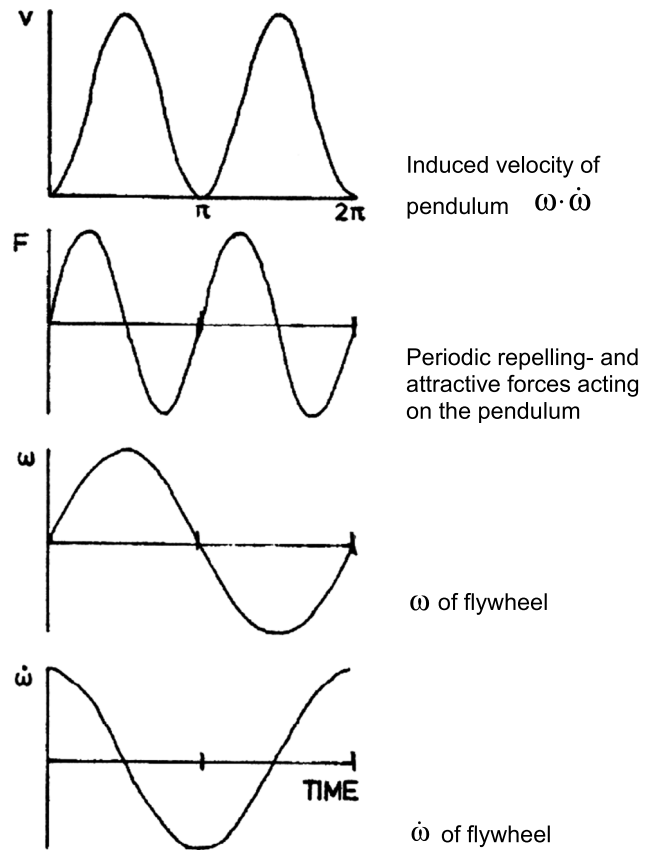


**Figure 7:** With respect to a full oscillation period of the flywheel, the measured velocity of the pendulum mirror, acting attractive and repelling forces, angular velocity and acceleration are vertically arranged. The x-axis is the time axis. A force proportional to  $\omega \cdot \dot{\omega}$  seems to be responsible for this behaviour.

measured acceleration is higher. With an estimated maximum velocity of the pendulum masses of  $10^{-5} \text{ m/s}$ , the accelerations must be of the order of  $10^{-6} \text{ m/s}^2$ .

In the vein of the assumptions above, the measured repelling acceleration hints to a cross-section of the order of  $1\text{b}$ .

## 5 Conclusion

In conclusion, it is conjectured that

- periodically accelerating and decelerating force effects have become visible in these experiments, *i.e.*,
- the DTQs emitted in the frame of energy conservation can be responsible for the force,
- the DTQs seem to establish an energy flow into or from the space during energy conservation processes, which are measurable by means of interacting forces,

- the force does not only affect the pendulum weight but also the gas content in the vessel, which leads to an imprinted gas flow at the end of experiment,
- the negative result of the lead-shielding experiment (see Section 4.2.2) hints to an “Open force” situation, where forces go beyond the area of the interaction experiment
- the measurements are based on the periodicity of the DTQ-source in the flywheel process, which gives first reliable information about the chronology and the strength of the Doppler force.

In ref. [10], an interesting experiment is reported that is based on a superconducting flywheel, which shows relatively strong effects in nearby located laser gyroscopes. These signals could be registered only during the phase of angular acceleration or deceleration. The interpretation as a gravitomagnetic effect seems many orders high as it could be in accordance with the Lense–Thirring effect (a factor of  $10^{23}$  discrepancy to be a gravitomagnetic effect) [11]. Since the gyroscope measure only affects the acceleration and deceleration phases of the flywheel, it seems that DTQs can be responsible for this effect.

## 6 Outlook

A final remark concerns the properties of the DTQ pool. Since even extreme high-energy conservation processes will take place in nuclear reactions as well as in collision processes in high energy particle interactions, the pool seems to be filled even with the highest DTQ energies isotropically and of course with high density. This is reminiscent of the zero-point radiation of electromagnetic waves in QED as was described for the first time by H.G. Casimir in 1940 [12]. Note that the energy content of the zero-point radiation is unlimited provided that there is no cut-off frequency assumed as, for example, resulting from the Planck length. Note that DTQs are different from electromagnetic waves as, for instance, they are not screened but penetrate a sheet of lead. In addition to the zero-point radiation, it seems that we have to deal at any position of the space with an isotropic distribution of DTQ energies that penetrate a probe.

In the future, the research has to focus on replicating the experiments described here and the improvement of the sensitivity of the detection system. Experiments with

periodic acceleration/deceleration processes should be preferred since the interpretation is optimally reliable. The lack of calibration and concern for direction and strength of force should then be resolved in future experiments.

**Acknowledgements:** The author would like to express his gratitude to Anselm Citron for supporting the theoretical work as well as to Vincent Schultheiß, who made valuable contributions during the final reading of the draft.

**Funding information:** The author states no funding involved.

**Author contributions:** The author has accepted responsibility for the entire content of this manuscript and approved its submission.

**Conflict of interest:** The author states no conflict of interest.

## References

- [1] Mößbauer R. Gammastrahlung in Ir191. *Z Phys.* 1958;151:124–43. doi: 10.1007/BF01344210.
- [2] Schrödinger E. Dopplerprinzip und Bohrsche Frequenzbedingung. *Phys Z.* 1922;23:301.
- [3] Cantor W. Equivalence of Compton effect and Doppler effect. *Stroboscopic Lett.* 1971;4(3 & 4):59.
- [4] Kidd R, Ardini J, Anton A. Compton effect as a double Doppler shift. *Am J Phys.* 1985;53(7):641.
- [5] Lemons DS. Doppler shift and stellar aberration from conservation laws applied to Compton shift. *Am J Phys.* 1991;59(11):1046.
- [6] Wilkins D. A new angle on Compton scattering. *Am J Phys.* 1992;60(3):221.
- [7] Ashwood DJG, Jennison JGRC. The scattering of an electromagnetic wave by a free electron. *J Phys A: Math Nucl Gen.* 1994;7(7):803.
- [8] Schultheiss C. Mass attraction caused by ultralong-wave photons? *Adv Stud Theor Phys.* 2008;2(10):491–505.
- [9] Schultheiss C. Momentum and energy of a mass consisting of a confined photon and resulting quantum-mechanical implications. *Adv Stud Theor Phys.* 2013;7(9–12):555–83.
- [10] Tajmar M, Plesescu F, Seifert B, Marhold K. La Crosse viral infection in hospitalized pediatric patients in Western North Carolina. *AIP Conf Proc.* 2007;880:1071–42. doi: 10.1063/1.2437552.
- [11] Graham RD, Hurst RB, Thirkettle RJ, Rowe CH, Butler PH. Experiment to detect frame dragging in a lead superconductor. *Phys C: Supercond Appl.* 2008;468(5(1)):383–7.
- [12] Casimir HBG. On the attraction between two perfectly conducting plates. *Koinkl Ned Akad Wetens Sect Proc.* 1948;51:793.